









PROBING JUPITER–SATELLITE INTERACTIONS FROM THE BEAMING OF THEIR DECAMETRIC EMISSIONS: THE CASE OF EUROPA AND GANYMEDE

L. Lamy^{1,2,3*} , A. Duchêne³, E. Mauduit¹ ,
P. Zarka^{1,2} , S. Yerin^{4,5} , C. K. Louis⁶ ,
J.-M. Griessmeier^{7,2} , J. Girard^{1,2} , and G. Theureau^{7,8,2} 

*Corresponding author: laurent.lamy@obspm.fr

Citation:

Lamy et al., 2023, Probing Jupiter–satellite interactions from the beaming of their decametric emissions: The case of Europa and Ganymede, *in Planetary, Solar and Heliospheric Radio Emissions IX*, edited by C. K. Louis, C. M. Jackman, G. Fischer, A. H. Sulaiman, P. Zucca, published by DIAS, TCD, pp. 267–277, doi: 10.25546/103097

Abstract

In a recent study, we accurately measured the beaming of Io–Jupiter decametric emissions, whose uncertainty is controlled by that on the position of the active Io flux tube (IFT) hosting the radiosources. The active IFT was positioned by 3 different methods using either simultaneous radio/UV measurements, either bi-point radio measurements, or independent models of equatorial lead angle. We found largely oblique beaming angles θ within $70 - 80^\circ$ from the local magnetic field vector, decreasing with increasing frequency. Assuming that Io–Jupiter radio emissions are driven by the electron cyclotron maser from loss cone electron distribution functions, we then derived the kinetic energy of unstable electrons E_{e-} associated to each time–frequency measurement of Io–Jupiter decametric arcs, ranging from

¹ LESIA, Observatoire de Paris, Université PSL, CNRS, Sorbonne Université, Université de Paris, Meudon, France

² Observatoire de Radioastronomie de Nançay, Observatoire de Paris, Université PSL, CNRS, Univ. Orléans, Nançay, France

³ Aix Marseille Univ, CNRS, CNES, LAM, Marseille, France

⁴ Institute of Radio Astronomy of NAS of Ukraine, Kharkiv, Ukraine

⁵ V. N. Karazin Kharkiv National University, Kharkiv, Ukraine

⁶ Dublin Institute for Advanced Studies, Dunsink Observatory, Dublin, Ireland

⁷ LPC2E, CNRS, Université d'Orléans, Orléans, France

⁸ LUTh, Observatoire de Paris, Université PSL, CNRS, Sorbonne Université, Université de Paris, Meudon, France

3 to 16 keV. Both θ and E_{e-} were found to significantly vary as a function of the altitude along the field line and, independently, as a function of time. In this follow-up study, we employ the same approach to study a sample of the recently discovered Europa- and Ganymede-Jupiter decametric emissions, as observed from the Nançay Decameter Array (NDA) and NenuFAR in Nançay. Interestingly, we measure θ and E_{e-} which strikingly compare to those obtained for the Io-Jupiter decametric events, promoting common acceleration and radio emission processes for the three planet-moon interactions.

1 Introduction

The electrodynamic interaction between Jupiter and Io has long been known to drive powerful, highly elliptically polarized, anisotropic decametric (DAM) emissions ranging from ~ 1 MHz to 40 MHz, which appear as arc-shaped structures in the time-frequency plane (Bigg, 1966; Zarka et al., 2001). These Io-DAM arcs have been historically classified into 4 main categories, depending on their sense of curvature (labelled B and D for vertex-early, A and C for vertex-late) and their sign of circular polarization (A and B for right-handed - RH - northern sources, C and D for left-handed - LH - southern ones Marques et al., 2017). Io-DAM has early been suspected to be eXtraordinary (X) mode emission amplified at the local electron cyclotron frequency f_{ce} by the Cyclotron Maser Instability (CMI) from loss cone electron distribution functions of a few keV (Hess et al., 2008a,b). In a recent study, Lamy et al. (2022b) developed a method aimed at determining (i) the Io-DAM beaming angle θ relative to the local magnetic field vector at the source and, assuming loss cone-driven CMI, (ii) the corresponding kinetic energy of CMI-unstable electrons E_{e-} . By using an up-to-date, Juno-derived, magnetic field model, the authors showed that the uncertainty on θ mainly depends on the uncertainty on the position of the active Io flux tube (IFT) hosting the Io-DAM sources. They presented 3 methods to position the active IFT using simultaneous radio/UV measurements, bi-point radio measurements and independent models of equatorial lead angle. By analyzing 11 cases of Io-DAM arcs observed by the Nançay Decameter Array (NDA), NenuFAR and Juno, they found largely oblique beaming angles $\theta \sim 70 - 80^\circ$, decreasing with increasing frequency, and associated $E_{e-} \sim 3 - 16$ keV. Both θ and E_{e-} were also found to significantly vary as a function of the frequency (which means as a function of the altitude along the field line) and, independently, as a function of time (or equivalently as a function of Io's longitude), suggesting strongly variable acceleration processes such as field-aligned potentials (Hess et al., 2007, 2009).

Similar radio emissions induced by Europa and Ganymede have been discovered recently, from the statistical analysis of long-term NDA observations between 10 and 40 MHz, then stacked into occurrence diagrams plotted as a function of the moon phase and the Central Meridian Longitude (CML Zarka et al., 2018; Jácome et al., 2022) and from the comparison between modeled and observed dynamic spectra from space-based observations of Voyager (up to 40 MHz) and Cassini (up to 16 MHz) (Louis et al., 2017b). Europa- and Ganymede-DAM (hereafter Eu- and Gan-DAM) emissions share basic properties with

the Io-DAM ones: they appear as arc-shaped structures with a high degree of circular polarization, so that they were classified with the same nomenclature. They are generally weaker and reach lower frequencies (median maximal frequency of ~ 22 MHz in the north and ~ 13 MHz in the south), as they result from less efficient planet–satellite interactions (Hess et al., 2011) and are associated with flux tubes whose maximal magnetic field amplitude near the Jovian ionosphere is generally less than for Io. This in turn makes them harder to disentangle from the rest of non-satellite (auroral) DAM emissions. Here, we present a study of a few clear cases of Eu- and Gan-DAM emissions tracked with the NDA and NenuFAR since 2016 and the arrival of Juno in orbit (Section 2). We then determine for the first time their beaming angle θ and infer the kinetic energy of associated CMI-unstable electrons E_{e-} along the approach developed for the case of Io (Section 3), before to end with perspectives (Section 4).

2 Search for Europa– and Ganymede–Jupiter decametric arcs

2.1 Dataset

The radio observatory of Nançay (Sologne forest, France) hosts several low-frequency radiotelescopes, two of which provide regular decametric observations of Jupiter.

The NDA is observing Jupiter on a quasi-daily basis with twice 72 Tee-Pee antennas, sensitive to RH and LH polarization, respectively, and several digital receivers (Boischoth et al., 1980; Lamy et al., 2017). The Routine receiver is a swept-frequency spectrometer which provides survey observations at modest, $500 \text{ ms} \times 75 \text{ kHz}$, time–frequency resolution. The NDA/Routine Jupiter data collection is referenced as Lamy et al. (2021) and is publicly available in CDF format (Cecconi et al., 2020). The catalog of Jupiter emissions built from this dataset between 1990 and 2016 by Marques et al. (2017) has been recently extended up to 2021 by J acome et al. (2022). The NewRoutine receiver is a FFT-based spectrometer achieving multichannel simultaneous RH and LH measurements post-integrated at the $500 \text{ ms} \times 49 \text{ kHz}$ resolution, increasing the signal-to-noise ratio with respect to the Routine receiver by a factor of ~ 30 . The NDA/NewRoutine Jupiter data collection is referenced as Lamy et al. (2022a) and is about to be publicly released in FITS format (Duchene et al., 2022).

NenuFAR is a giant phased array in Nançay (Zarka et al., 2020). As part of the early science phase which extended from mid-2019 to late 2022, NenuFAR regularly observed Jupiter in support of Juno through a dedicated Jupiter Key Project. During this construction phase, the number of NenuFAR mini-arrays (each made of 19 crossed-dipoles), and therefore the total effective area, regularly increased, rapidly overcoming the NDA sensitivity. Survey observations of Jupiter were obtained near each Juno perijove with the UnDySPuTeD receiver (Bondonneau et al., 2021), which provides the full Stokes parameters. For our purpose, it was configured to observe the 10-40 MHz range with a 84 ms temporal cadence and linearly-spaced frequency channels every 12.2 kHz. To facilitate the search for events of interest, we catalogued separately all individual features in these NenuFAR Jupiter observations.

For the purpose of comparison with those radio observations, we also used polar projections of the Jovian UV aurorae imaged by the Hubble Space Telescope (HST) through the APIS service (Lamy et al., 2015) to catalog the UV footprint of Jupiter’s moons.

2.2 Identification of Eu- and Gan-DAM events

To search for Jovian DAM emissions associated with either Europa or Ganymede, we built up on the approach described above for Io. We focussed on the 2016-2021 interval, which coincided with in-orbit measurements of the Juno mission.

2.2.1 Simultaneous radio/UV measurements

Assuming a magnetic conjugacy between the radio sources and the ultraviolet auroral footprint for both moons, we first cross-matched the HST catalog of UV footprints with the NDA and NenuFAR catalogs of Jupiter radio emissions. Unfortunately, we could not identify any moon-related emission simultaneously observed at both wavelengths.

2.2.2 Stand-alone radio observations

We thus searched for individual events in stand-alone radio observations of both instruments. The recent detection of Eu- and Gan-DAM components has motivated the development of an online Jupiter probability tool at <https://jupiter-probability-tool.obspm.fr> which enables one to check the occurrence probability of radio emissions driven by Io, Europa and/or Ganymede for any observing time interval (Cecconi et al., 2023). It is therefore straightforward to identify individual radio arcs consistently related to one satellite and inconsistent with the other ones. This approach was already used by Mauduit et al. (2023) to constrain the origin of the DAM emissions recorded by the NDA at very high resolution in April 2021, which yielded the identification of several Gan-DAM bursts. We used this tool similarly to achieve a list of Eu- and Gan-DAM plausible emissions among the arcs cataloged from NDA and NenuFAR observations between 2016 and 2021. Hereafter, we present 4 of the most convincing candidates.

Figure 1a₁-c₁ displays three cases of isolated decametric arcs observed by the NDA/New-Routine receiver. Their time interval, marked by a double arrow, is mapped onto the Ganymede (phase, CML) diagram obtained by Zarka et al. (2018) on Figure 1a₂-c₂. Figure 1a-b display two cases of Gan-DAM arcs on 7th and 17th April 2021 already identified by Mauduit et al. (2023). The occurrence coincides with the Gan-B (Gan-C, resp.) most probable region in the (phase, CML) diagram, while being inconsistent with other satellites. The vertex-late curvature, RH (LH, resp.) polarization and high-frequency limit of 21 MHz (19 MHz, resp.) is also consistent with the Gan-B emission properties (Gan-C, resp.). Figure 1c displays a third, weak, vertex-late and RH-polarized arc visible on 31st March 2017 between 13 and 22 MHz. Its time interval and characteristics here correspond to a Gan-A emission (only).

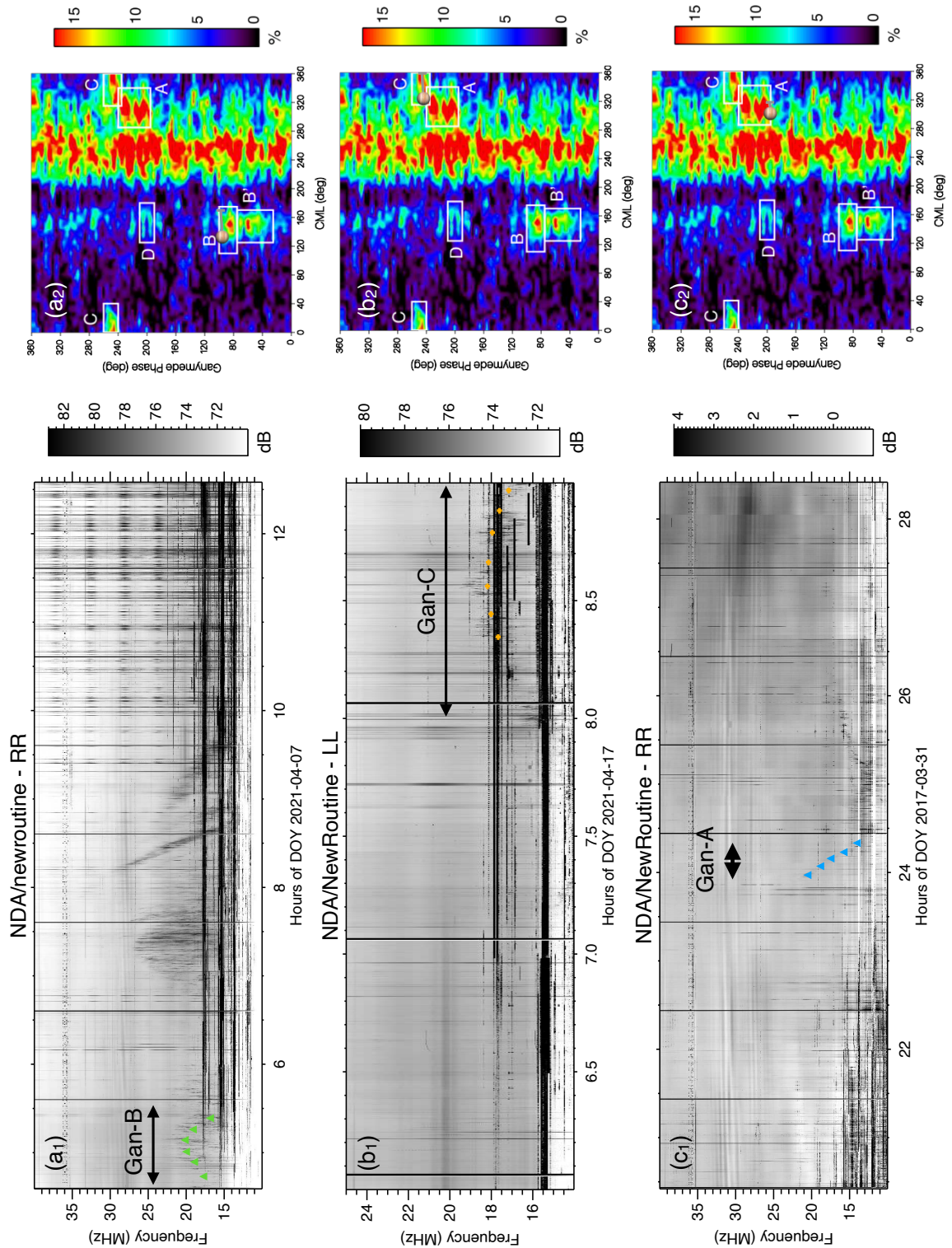


Figure 1: (a₁-b₁-c₁) NDA/NewRoutine dynamic spectra of RH- or LH-polarized (referred to as RR and LL) flux density ($V^2 m^{-2} Hz^{-1}$ expressed in dB) showing isolated Jovian decametric arcs below 22 MHz, fitted by colored symbols. In the specific case of panel c₁, a medium background was subtracted to each spectrum to improve the contrast of the weak RH arc fitted by blue triangles. (a₂-b₂-c₂) Ganymede (phase, CML) occurrence diagram (Zarka et al., 2018). The gray curve (in the white box) marked by the Jupiter logo maps the time interval corresponding to the arc identified on the left-hand side (double arrow).

Figure 2 displays a NenuFAR/UnDySPuTeD observation of Jupiter executed on 14th April 2021 with two dynamic spectra of the flux density and of the degree of circular polarization. A series of intense, RH-polarized, vertex-late arcs reaching frequencies as high as 27 MHz is visible on both panels and indicate northern, duskside, emissions of auroral origin (unrelated to moons). Indeed, while the 05:00-07:00 interval intercepts both the Io-B and Gan-B most probable regions in the Io and Ganymede (phase, CML) diagrams (unshown), such B-type emissions should correspond to isolated, RH-polarized, vertex-early arcs not seen here. Near 04:30, instead, a fainter, LH-polarized (black color), vertex-late arc extending from 10 to 17 MHz is visible in Figure 2b only. This illustrates the value of searching for circularly polarized emissions in V-stokes dynamic spectra, for which the signal-to-noise ratio is improved, especially in the low-frequency range contaminated by radio frequency interferences (RFI). The arc is fitted by purple triangles. Its time interval, ranging from 04:15 to 04:45 (double arrow) coincides with the Eu-C most probable region displayed in Figure 2c, as derived from Voyager/Cassini observations (Louis et al., 2017b). It is worth reminding that the Eu-C region identified from

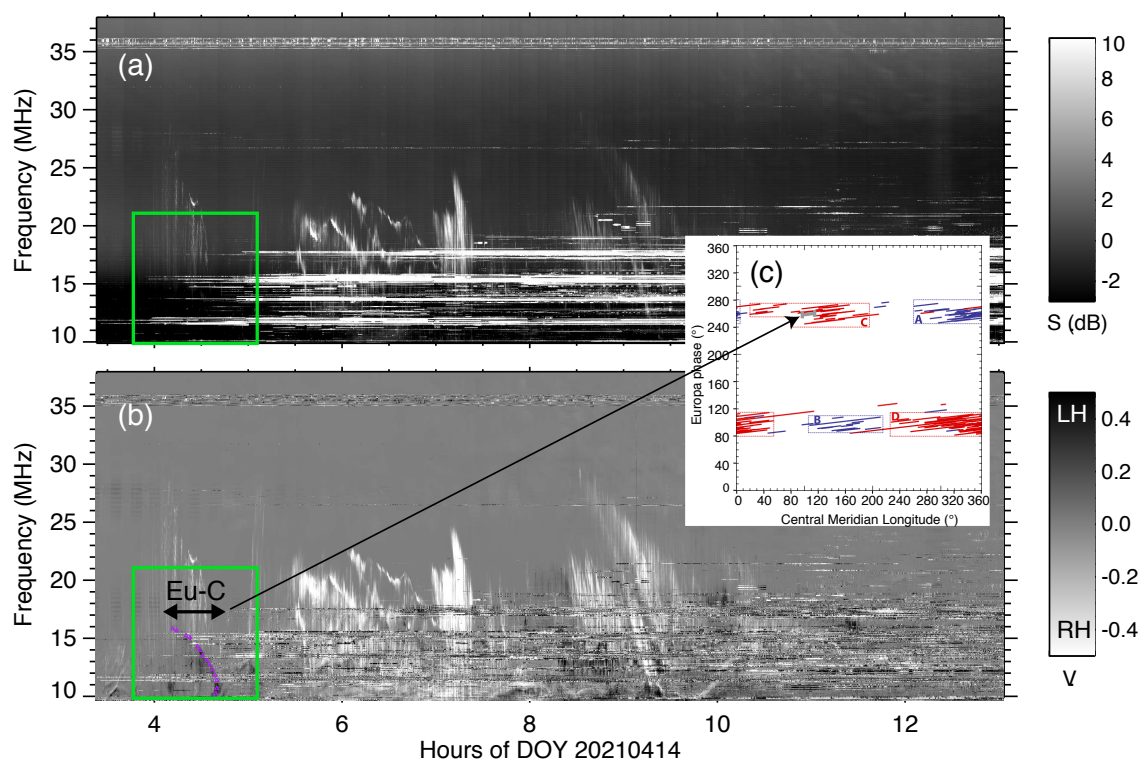


Figure 2: NenuFAR/UnDySPuTeD dynamic spectrum of (a) flux density and (b) degree of circular polarization showing Jovian decametric emissions on 14th April 2021. The green rectangles indicate a faint, vertex-late, LH-polarized arc (black color) visible only in the V-Stokes dynamic spectrum. This arc is fitted with purple triangles. (c) Europa (phase, CML) occurrence diagram (Louis et al., 2017b). The gray curve, which intercepts the Eu-C box, again maps the time interval corresponding to the arc identified on the left-hand side (double arrow).

Cassini/Voyager does not coincide with that derived from NDA/Routine observations, probably because of different sensitivity, spectral range and RFI for those instruments. However, the NenuFAR high sensitivity and spectral resolution makes it easier to track faint, low-frequency, circularly polarized arcs.

Overall, we consider the above-described four candidates of Eu- and Gan-DAM arcs as reliable. An unambiguous confirmation would deserve multi-point radio measurements of the same emission with a time delay corresponding to the time interval needed by a given source to illuminate both observers successively, hence tied with the satellite revolution period (see examples in the case of Io in Louis et al. (2017a)). Unfortunately, this time delay can be long for largely separated observers (such as Nançay and Juno), longer than the emission temporal variability, so that we could not confirm those candidates with Juno/Waves radio observations. However, the probability that a given radio arc intercepts exactly a given satellite (phase, CML) region is very low. In addition, we are hereafter interested in average characteristics of those arcs taken altogether so that even one false detection would marginally change the results presented in the next section.

Once these Eu- and Gan-DAM arcs identified, we analyzed them with the method developed by Lamy et al. (2022b) for the Io-DAM emissions. We first fitted the time–frequency profile of each arc (as displayed by colored symbols in Figures 1-2). We then positioned the corresponding radio sources at $f = f_{ce}$ all along the Europa and Ganymede active flux tubes, as derived from the Juno JRM09 + current sheet magnetic field model (Connerney et al., 2018, 2020) and from the Europa and Ganymede lead angle models (displayed in Figure 3) which we built from HST statistical observations measurements of the Europa and Ganymede UV footprints fitted by Bonfond et al. (2017). We finally determined (1) the aperture angle $\theta(f) = (\mathbf{k}, \mathbf{B})$ (\mathbf{k} the wave vector at the source, \mathbf{B} the local magnetic field vector counted positively outwards) assuming straight-line propagation and (2) the kinetic energy of CMI-unstable loss cone electrons E_{e-} (obtained from θ with the Equation (4) from Hess et al. (2008a)) for each time–frequency measurement. We remind here that the uncertainty on θ is controlled by that on the position of the active flux tube rather than that on the fit itself. Also, while the footpath of Europa and Ganymede measured by Bonfond et al. (2017) are not continuous in longitude, the observed time intervals corresponded to a valid portion of these models.

3 Beaming angle and associated electron kinetic energy

Figure 4 provides the results of this analysis, in a format directly comparable to Figure 11 of Lamy et al. (2022b) for Io. Despite the low number of Eu- and Gan-DAM events analyzed here, Figure 4a displays results very similar to those obtained for Io-DAM arcs. Figure 4a displays strongly oblique beaming angles θ within $71 - 87^\circ$, which decrease with increasing frequency in two cases (as expected for loss-cone driven CMI emission with a constant energy of unstable electrons) and show a more complex shape in the other two cases. In Figure 4b, the associated values of E_{e-} vary between 0.5 and 15 keV with a strong variability. For the Gan-C event of Figure 1b (corresponding to the orange symbols in Figure 4b), the frequency of the arc (altitude of the sources) was nearly constant, so that the observed variation of θ and E_{e-} can be unambiguously attributed to a variation in time (or longitude of Ganymede).

More generally, the derived values of θ and E_{e-} compare well with the $\sim 70 - 80^\circ$ and $\sim 3 - 16$ keV ranges obtained for Io-DAM events. This similarity both strengthens this

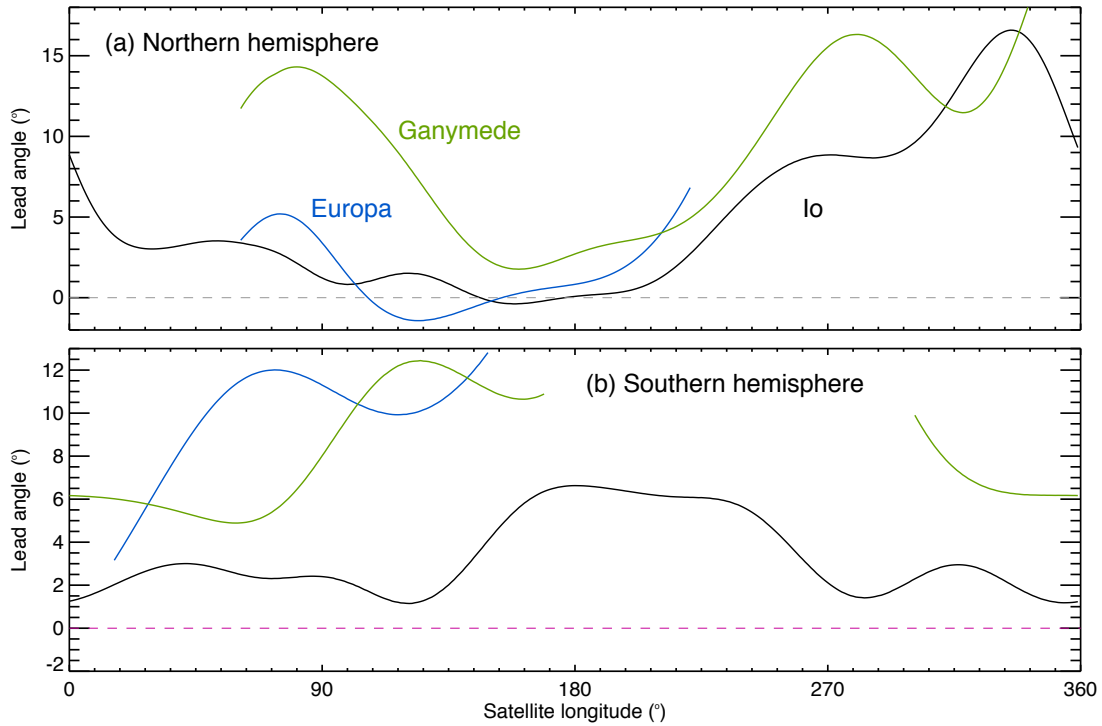


Figure 3: Equatorial lead angle models of the Io (black), Europa (blue) and Ganymede (green) flux tube derived from the Juno JRM09+current sheet magnetic field model applied to the HST statistical observations measurements of satellite UV footprints fitted by Bonfond et al. (2017).

analysis and suggests that the acceleration and radio emission conditions are similar for the three types of Jupiter–moon electrodynamic interactions.

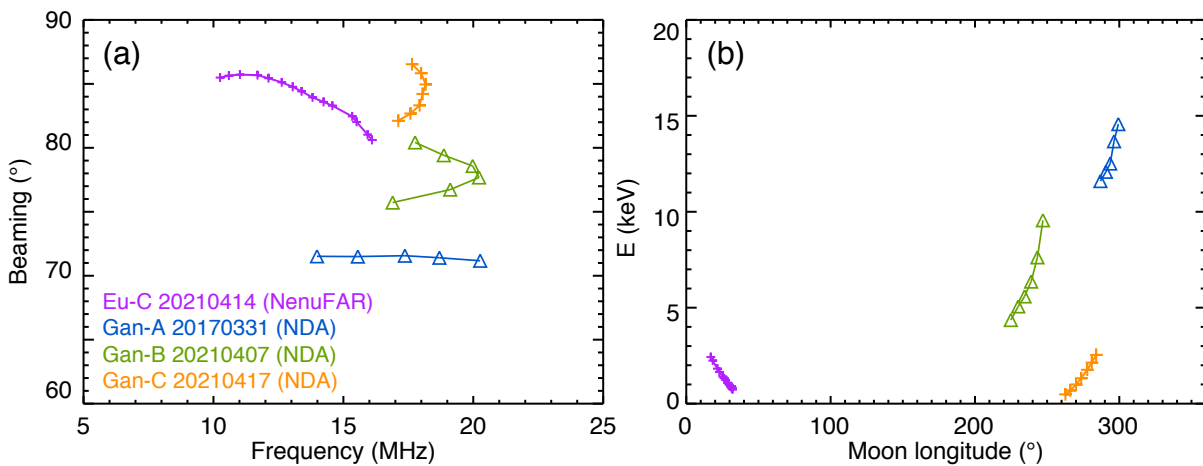


Figure 4: (a) Beaming angle θ as a function of frequency for 4 cases of Europa– and Ganymede–Jupiter decametric emissions. (b) Inferred electron kinetic energy E_{e^-} as a function of the moon’s longitude. This figure directly compares to Figure 11 of Lamy et al. (2022b).

4 Conclusions and perspectives

In this study, we have identified four cases of Eu- and Gan-DAM emissions in long-term NDA/NewRoutine and NenuFAR/UnDySPuTeD observations of Jupiter. By adapting a method recently developed to investigate Io-DAM emissions, we determined their beaming angle at the source $\theta \sim 71-87^\circ$ and inferred the associated kinetic energy of CMI-unstable loss cone electrons $E_{e-} \sim 0.5 - 15$ keV. Interestingly, these results compare well to those obtained for Io-DAM events. This suggests that common, likely universal, acceleration and radio emission conditions are controlling the physical ionosphere-magnetosphere coupling processes along the three moons magnetic flux tubes. While the limited number of analyzed cases prevents from statistically analyzing those characteristics, in the case of one Gan-DAM arc at least, we showed evidence of a temporal variability of θ and E_{e-} associated with a Jupiter-moon variable interaction. The statistical application of this analysis, taking full advantage of long-term NDA, NenuFAR and Juno radio observations forms a rich perspective to this work.

Acknowledgments:

The authors thank both referees for their valuable and constructive comments. The authors acknowledge support from CNES and from CNRS/INSU programs of Planetary (PNP) and Heliophysics (PNST). The NDA data are released at <https://www.obs-nancay.fr/reseau-decametrique/>. The NenuFAR data are accessible on demand to the PIs of key projects. The HST processed observations were provided by the APIS CNRS/INSU observation service <http://apis.obspm.fr> hosted by the Paris Astronomical Data Centre at Observatoire de Paris (Lamy & Henry, 2021). LL thanks Rose Dumont and Esteban Servajean who have respectively catalogued the HST polar projections of Jupiter and the NenuFAR observations of Jupiter during their short internship aimed at discovering the world of research. The authors thank B. Cecconi, P. Renaud and A. Loh for their work on the production of NDA and NenuFAR data, and M. Marques for sharing the NDA/Jupiter catalog. C. K. Louis was funded by the Science Foundation Ireland Grant 18/FRL/6199.

References

- Bigg E. K., 1966, Periodicities in Jupiter's decametric radiation, *Planet. & Space Sci.*, *14*, 741
- Boischot A., et al., 1980, A new high-grain, broadband, steerable array to study Jovian decametric emission, *Icarus*, *43*, 399
- Bondonneau L., et al., 2021, Pulsars with NenuFAR: Backend and pipelines, *Astron. & Astrophys.*, *652*, A34

- Bonfond B., Saur J., Grodent D., Badman S. V., Bisikalo D., Shematovich V., Gérard J. C., Radioti A., 2017, The tails of the satellite auroral footprints at Jupiter, *Journal of Geophysical Research (Space Physics)*, *122*, 7985
- Cecconi B., Coffre A., Loh A., Denis L., Lamy L., 2020, ORN NDA Routine Jupiter EDR CDF Dataset Specification, doi:10.25935/2EAP-W742, <https://doi.org/10.25935/2EAP-W742>
- Cecconi B., Aicardi S., Lamy L., 2023, Jupiter radio emission probability tool, *Frontiers in Astronomy and Space Sciences*, *10*
- Connerney J. E. P., et al., 2018, A New Model of Jupiter's Magnetic Field From Juno's First Nine Orbits, *Geophys. Res. Lett.*, *45*, 2590
- Connerney J. E. P., Timmins S., Hecceg M., Joergensen J. L., 2020, A Jovian Magnetodisc Model for the Juno Era, *Journal of Geophysical Research (Space Physics)*, *125*, e28138
- Duchene A., Lamy L., Loh A., Cecconi B., Viou C., Renaud P., 2022, ORN NDA New Routine Jupiter EDR FITS Dataset Specification, doi:10.25935/MPF0-V756, <https://doi.org/10.25935/MPF0-V756>
- Hess S., Zarka P., Mottez F., 2007, Io Jupiter interaction, millisecond bursts and field-aligned potentials, *Planet. & Space Sci.*, *55*, 89
- Hess S., Cecconi B., Zarka P., 2008a, Modeling of Io–Jupiter decameter arcs, emission beaming and energy source, *Geophys. Res. Lett.*, *35*, L13107
- Hess S., Mottez F., Zarka P., Chust T., 2008b, Generation of the Jovian radio decametric arcs from the Io Flux Tube, *Journal of Geophysical Research (Space Physics)*, *113*, A03209
- Hess S., Mottez F., Zarka P., 2009, Effect of electric potential structures on Jovian S-burst morphology, *Geophys. Res. Lett.*, *36*, L14101
- Hess S. L. G., Delamere P. A., Dols V., Ray L. C., 2011, Comparative study of the power transferred from satellite–magnetosphere interactions to auroral emissions, *Journal of Geophysical Research (Space Physics)*, *116*, A01202
- Jácome H. R. P., Marques M. S., Zarka P., Echer E., Lamy L., Louis C. K., 2022, Search for Jovian decametric emission induced by Europa on the extensive Nançay Decameter Array catalog, *Astron. & Astrophys.*, *665*, A67
- Lamy L., Henry F., 2021, APIS/HST data collection, doi:10.25935/T184-3B87, <https://doi.org/10.25935/T184-3B87>
- Lamy L., Prangé R., Henry F., Le Sidaner P., 2015, The Auroral Planetary Imaging and Spectroscopy (APIS) service, *Astronomy and Computing*, *11*, 138

- Lamy L., Zarka P., Cecconi B., Klein L., Masson S., Denis L., Coffre A., Viou C., 2017, 1977-2017: 40 years of decametric observations of Jupiter and the Sun with the Nançay Decameter Array, in *Planetary Radio Emissions VIII*, eds Fischer G., Mann G., Panchenko M., and Zarka P., pp 455–466, doi:10.1553/PRE8s455
- Lamy L., et al., 2021, Nançay Decameter Array (NDA) Jupiter Routine observation data collection, doi:10.25935/DV2F-X016, <https://doi.org/10.25935/DV2F-X016>
- Lamy L., et al., 2022a, Nançay Decameter Array (NDA) Jupiter NewRoutine observation data collection, doi:10.25935/7zcg-8e29, <https://doi.org/10.25935/7zcg-8e29>
- Lamy L., et al., 2022b, Determining the Beaming of Io Decametric Emissions: A Remote Diagnostic to Probe the Io–Jupiter Interaction, *Journal of Geophysical Research (Space Physics)*, 127, e30160
- Louis C. K., et al., 2017a, Io–Jupiter decametric arcs observed by Juno/Waves compared to ExPRES simulations, *Geophys. Res. Lett.*, 44, 9225
- Louis C. K., Lamy L., Zarka P., Cecconi B., Hess S. L. G., 2017b, Detection of Jupiter decametric emissions controlled by Europa and Ganymede with Voyager/PRA and Cassini/RPWS, *Journal of Geophysical Research (Space Physics)*, 122, 9228
- Marques M. S., Zarka P., Echer E., Ryabov V. B., Alves M. V., Denis L., Coffre A., 2017, Statistical analysis of 26 yr of observations of decametric radio emissions from Jupiter, *Astron. & Astrophys.*, 604, A17
- Mauduit E., Zarka P., Lamy L., Hess S. L. G., 2023, Drifting discrete Jovian radio bursts reveal acceleration processes related to Ganymede and the main aurora, *Nature Communications*, 14, 5981
- Zarka P., Queinnec J., Crary F. J., 2001, Low-frequency limit of Jovian radio emissions and implications on source locations and Io plasma wake, *Planet. & Space Sci.*, 49, 1137
- Zarka P., Marques M. S., Louis C., Ryabov V. B., Lamy L., Echer E., Cecconi B., 2018, Jupiter radio emission induced by Ganymede and consequences for the radio detection of exoplanets, *Astron. & Astrophys.*, 618, A84
- Zarka et al. 2020, The low-frequency radio telescope NenuFAR, in *Proceedings of the URSI GASS 2020 conference hold in Rome 29/8-5/9/2020*, pp 1–4